Bull. Astr. Soc. India (1996) 24, 103-116

How are the observed frequencies related to solar structure?

Jørgen Christensen-Dalsgaard

Teoretisk Astrofysik Center, and Institut for Fysik og Astronomi, Aarhus Universitet, DK-8000 Aarhus C, Denmark

Abstract. The frequencies of the solar five-minute oscillations are largely determined by the variation of sound speed and density with radius; of these, the dependence on sound speed dominates and can be understood in terms of the asymptotic description of the modes. Additional, so far uncertain, contributions are introduced in the near-surface region by nonadiabaticity and by the dynamical effects of convection; however, these contributions can to a large extent be suppressed in the analysis of the frequencies. The structure of the model, and hence the frequencies, are in turn determined by the physics and other assumptions used in the computation of the solar models. In particular, the frequencies provide sensitive measures of the equation of state and opacity of matter in the Sun, and give clear evidence for the importance of settling and diffusion of helium and heavy elements beneath the solar convection zone.

Key words: Sun: structure — Sun: oscillations — helioseismology

1. Introduction

The observed solar frequencies offer an unprecedented amount of accurate data relating to the structure of stellar interior. The most precise frequencies are known with a a relative standard deviation of less than 5×10^{-6}, better by a factor of more than 10 than the most precise value of the gravitational constant and hence the solar mass. Furthermore, the nature of the observed modes permits inversion to relate the frequencies to the structure of localized regions of the Sun, extending from the solar core to near its surface. As a result, we can now test the theory of stellar evolution, as applied to the case of the present Sun, with great precision and detail.

With a few exceptions, it may be argued that the the actual solar structure is of relatively little interest. The depth of the solar convection zone, determined from helioseismology with considerable precision (*e.g.* Christensen-Dalsgaard, Gough & Thompson

1991) is of importance to the study of the dynamics of the convection zone and the theory of the solar dynamo. Also, a knowledge of solar structure is required for inversion to determine the solar rotation, and other departures from spherical symmetry. Apart from such applications, however, the principle goal of helioseismic studies of solar structure is to investigate the assumptions and physics underlying calculations of solar evolution.

2. Properties of solar modelling

The assumptions and physical properties used in stellar evolution studies can conveniently if somewhat arbitrary, be divided into *macrophysics* and *microphysics*. The former establishes the general physical picture of the star, usually rather simplified, and hence defines the overall equations of stellar evolution that are considered. Given that, the microphysics provides the specific description of the properties of stellar matter required to carry out the detailed modelling.

The macrophysics concerns the overall state of equilibrium of the star and its gradual change as the star evolves due to nuclear transformation of composition and other possible processes which might effect the composition profile. It is useful to discuss these aspects in some detail.

2.1 Hydrostatic equilibrium

This involves the assumption of a balance of forces on the matter in the star. Any violation would lead to motion on a dynamical time scale which (apart from the oscillations and convection) is generally not observed. The basic equilibrium is between the gradient of pressure p and the force of gravity; assuming spherical symmetry, as I shall do in the following, this may be expressed as

$$\frac{\mathrm{d}p}{\mathrm{d}r} = -g\rho \,, \tag{1}$$

where r is distance from the centre, g is gravitational acceleration and ρ is density. Here it is usually assumed that p can be identified with the thermodynamic pressure (which includes contributions from both material particles and radiation), related to ρ, temperature T and composition through *an equation of state*. The latter depends on the description of the thermodynamic state and hence constitutes one part of the microphysics.

Equation (1) neglects possible sources other than gravity which might contribute to the balance of forces. One such contribution arises from the momentum transport resulting from the convective motion in stellar convection zones. This is often described in terms of a *turbulent pressure* $p_{\rm turb}$ which is included in eq. (1) by expressing p as $p = p_{\rm gas} + p_{\rm turb}$, where $p_{\rm gas}$ is the thermodynamic component. The behaviour of $p_{\rm turb}$ depends on the detailed description of convection, which is highly uncertain; however, it seems well established that $p_{\rm turb}$ is unlikely to make a significant contribution except in the outermost part of the outer convection zones, where the low density forces large convective velocities. Here, on the other hand, $p_{\rm turb}$ may contribute a substantial fraction of the total pressure. Another contribution to eq. (1) could arise from magnetic fields. In

this case, also, it seems plausible that the contribution is significant only in the superficial layers, unless the Sun were to have an exceedingly strong magnetic field. At the base of the convection zone, for example, a field of 10^6 gauss would contribute a magnetic pressure of only 7×10^{-4} of $p_{\rm gas}$. In contrast, the magnetic field, and possibly momentum transport by waves, make significant contributions to the pressure balance in the solar atmosphere, quite likely dominant in the upper parts of the atmosphere.

2.2 Energy transport

The transport of energy through the star depends, basically speaking, on the temperature gradient. Except in the stellar atmosphere the radiative flux is determined by the diffusion approximation:

$$F_{\rm rad} = -\frac{4a\tilde{c}T^3}{3\kappa\rho}\frac{{\rm d}T}{{\rm d}r}\,, \tag{2}$$

where a is the radiation density constant, $\tilde{c}$ is the speed of light, T is temperature, and κ is opacity. In convectively unstable regions, most of the energy is generally assumed to be carried by convection. Outside regions of composition gradients the condition for convective instability is normally expressed as

$$\nabla_{\rm rad} > \nabla_{\rm ad}\,, \tag{3}$$

where $\nabla_{\rm ad} = (\partial \ln T/\partial \ln p)_s$, the derivative being at constant specific entropy s; $\nabla_{\rm rad}$ is that value of $\nabla = {\rm d}\ln T/{\rm d}\ln p$, the derivative being along conditions in the model, which would be required to transport by radiation the total flux $F = L/4\pi r^2$, L being the luminosity.

It is normally assumed that energy is transported only by radiation and convection. Thus, in convectively stable regions $\nabla = \nabla_{\rm rad}$ which is easily obtained from eqs (1) and (2) by setting $F = F_{\rm rad}$. The result clearly depends on the opacity which therefore constitutes another part of the microphysics. In convective regions the dependence of the flux on the temperature gradient depends on the description of convection which should, ideally, take into account the non-local nature of the convective motion. Simple scaling arguments suggest that the convective flux $F_{\rm con}$ satisfies $F_{\rm con} \propto \rho(\nabla - \nabla_{\rm ad})^{3/2}$, the constant of proportionality being such that $\nabla - \nabla_{\rm ad}$ is very small except in a thin region near the top of outer convection zones. The details of this strongly superadiabatic region depends on the treatment of convection. Detailed hydrodynamical simulations of the near-surface convection have been made (*e.g.* Stein & Nordlund 1989). However, in calculations of overall stellar models simplified descriptions of convection are used. These often involve at least one *a priori* unknown parameter which determines the efficacy of convection, and hence the magnitude and extent of the superadiabatic region; in mixing-length theory, for example, this is the mixing-length parameter $\alpha_{\rm c}$. The choice of this parameter essentially fixes the value of the specific entropy in the adiabatic part of the convection zone.

This picture is certainly oversimplified, however. Beneath the convection zone motion must penetrate for a certain distance, giving rise to a *negative* convective flux; hence

the temperature gradient must be steeper than otherwise, to produce a compensating increase in the radiative flux. Simple models (Schmitt, Rosner & Bohn 1984; Zahn 1991) suggest a region of nearly adiabatic stratification, followed by a sharp transition to the radiative gradient. The models make no definite prediction of the extent of this region, however. Although strict limits have been placed by helioseismology on this model in its simplest form (*e.g.* Basu, Antia & Narasimha 1994; Monteiro, Christensen-Dalsgaard & Thompson 1994) there is little doubt that the temperature gradient must be affected by convective penetration. At greater depths there have been suggestions of a possible contribution to energy transport by gravity waves induced by the penetration (*e.g.* Press & Rybicki 1981), although even rough estimates of the likely magnitude of this effect appear highly uncertain. Finally, it seems clear that purely radiative models are unable to account for the structure of the solar atmosphere, implying other sources of energy transport such as acoustic or magnetic waves.

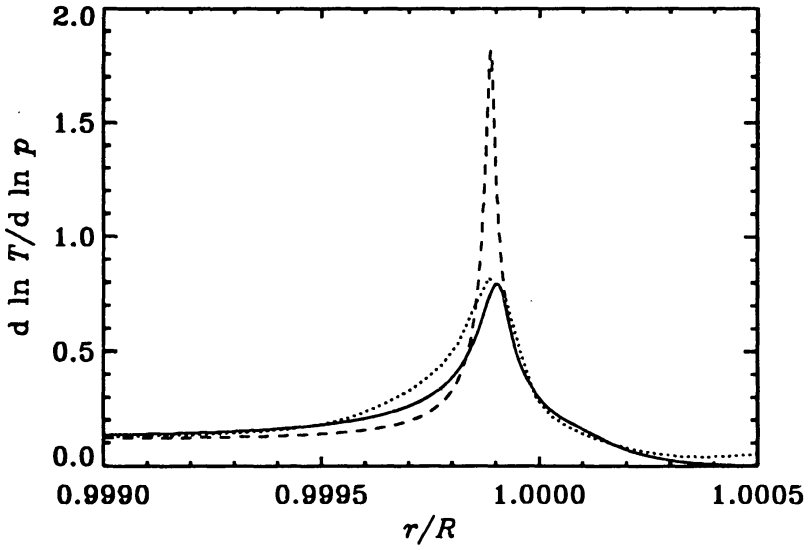

Figure 1. Temperature gradients in the near-surface region of solar models computed with the mixing-length theory (solid line) and the CM formulation (dashed line). The dotted line shows the average temperature gradient obtained in a hydrodynamical simulation of convection (*cf.* Stein & Nordlund 1989).

The structure of the strongly superadiabatic region near the surface depends on the assumed treatment of convection. In addition to mixing-length theory, a formulation based on second-order closure (Canuto & Mazzitelli 1991) has been used fairly extensively in recent years. The CM formulation is characterized by smaller efficiency where convective energy transport is relatively inefficient, leading to a steeper temperature gradient. This is evident from Fig. 1 which shows $\nabla - \nabla_{\rm ad}$ in a mixing-length model and a model using the CM formulation. For comparison, I also show the horizontally and temporally averaged gradient based on a three-dimensional hydrodynamical simulation of near-surface convection. Interestingly, the result of the simulation is similar to the mixing-length model.

2.3 Energy release

The energetics of a star is determined by the first law of thermodynamics, which may be written as

$$\frac{\mathrm{d}L}{\mathrm{d}r} = 4\pi r^2 \left[\rho\epsilon - \rho\frac{\mathrm{d}}{\mathrm{d}t}\left(\frac{u}{\rho}\right) + \frac{p}{\rho}\frac{\mathrm{d}\rho}{\mathrm{d}t}\right] ; \tag{4}$$

here ϵ is the rate of nuclear energy generation (reduced for the energy lost to neutrinos) per unit mass and time, and u is the internal energy per unit volume. The time-derivative terms arise from the change in thermodynamic state and the work of gravity. During main-sequence stellar evolution, which occurs on the time scale of hydrogen burning, these terms are very small. In a model of the present Sun, for example, their integrated contribution to the surface luminosity is around 0.01 %. In such a case the star is almost in thermal equilibrium. The nuclear energy generation rate and thermodynamic properties of the gas involved in eq. (4) are obviously parts of the microphysical description.

There have been suggestions of significant departures from thermal equilibrium for the present Sun (*e.g.* Dilke & Gough 1972). This would give rise to changes of solar structure on a thermal time scale, of order 10^6 years. Thus the immediately observable effects would be subtle; a detailed test of such models with the helioseismic data has so far not been carried out, however.

2.4 Change of composition

Within the framework of "classical" stellar evolution there are essentially two effects which may affect the composition of stellar interiors: nuclear reactions and microscopic gravitational settling and diffusion. Nuclear burning, fusing hydrogen into helium, controls the evolution of main-sequence stars such as the Sun. Settling and diffusion have been commonly ignored in calculations of stellar evolution, yet they are unavoidable unless counteracted by other processes (*e.g.* Noerdlinger 1977; Wambsganss 1988; Cox, Guzik & Kidman 1989). Within this picture the evolution of composition depends on nuclear reaction rates and diffusion and settling coefficients, which are obviously microphysical quantities. The structure of the present Sun depends on the profile of the hydrogen abundance by mass $X(m)$, m being the mass interior to a given point, which has resulted from the preceding evolution.

This description ignores the possible effects of macroscopic motion. Within the convection zones the time scales of motion are typically at most years, and hence the composition can be assumed to be perfectly homogeneous. In convectively stable regions the situation is less clear, however. The characteristic time scales for nuclear burning and gravitational settling are of the order of the age of the present Sun, and hence even quite weak motion can lead to significant mixing. That such mixing has taken place during some phase of solar evolution is evident from the fact that ^{7}Li has been depleted in the solar atmosphere by a factor of about 150 relative to the meteoritic abundance (*e.g.* Anders & Grevesse 1989). This requires mixing well beyond the bottom of the convection zone (*e.g.* Ahrens, Stix & Thorn 1992; Christensen-Dalsgaard, Gough & Thompson 1992). Such mixing might be caused by motion induced within the convection zone, in

the form of penetration (*cf.* Section 2.2), weaker turbulence or possibly gravity waves (Schatzman *et al.* 1981; Montalbán 1994). Also, rotationally induced circulation or instabilities associated with the spin-down from the often assumed state of initial rapid rotation may have led to some mixing, significantly changing the composition profile (*e.g.* Chaboyer, Demarque & Pinsonneault 1995).

3. Dependence of frequencies on solar structure

The modes of solar oscillation have sufficiently small amplitudes that they can be treated as linear perturbations around an equilibrium structure. They are characterized by the three wave numbers n, l and m. Of these, l and m determine the behaviour of the mode, given by a spherical harmonic Y_l^m, over spherical surfaces; the degree l is related to the total horizontal wave number k_h at the distance r from the centre by $k_h = \sqrt{l(l+1)}/r$, while m measures the number of nodes around the equator. Finally, n is essentially given by the number of nodes in the radial direction. For a spherically symmetric star, such as I consider here, the frequencies $\omega = \omega_{nl}$ are independent of m. In addition to the angular frequency ω, the cyclic frequency $\nu = \omega/(2\pi)$ is also commonly used.

In almost all the star the Lagrangian perturbations δp and $\delta\rho$ in pressure and density are related essentially adiabatically, *i.e.*, $\delta p/p \simeq \Gamma_1 \delta\rho/\rho$, where $\Gamma_1 = (\partial \ln p/\partial \ln \rho)_s$. Thus the computation of solar oscillations is often made in the adiabatic approximation, assuming this relation to hold exactly throughout the Sun. In that case, the oscillations are purely dynamical phenomena, and their frequencies are determined by the "mechanical" properties of the star, *viz.* p and ρ as functions of r, as well as $\Gamma_1(r)$. Furthermore, if hydrostatic equilibrium is assumed, p is related to ρ by eq. (1), using also Poisson's equation to determine g from ρ. In this case, therefore, the adiabatic oscillations are determined entirely by $\rho(r)$ and $\Gamma_1(r)$. Other, equivalent pairs of variables may be used; convenient choices are (c^2, ρ), $c^2 = \Gamma_1 p/\rho$ being the square of the adiabatic sound speed, or (A, Γ_1), where

$$A = \frac{1}{\Gamma_1}\frac{\mathrm{d}\ln p}{\mathrm{d}\ln r} - \frac{\mathrm{d}\ln\rho}{\mathrm{d}\ln r} \tag{5}$$

is the coefficient of convective stability.

In the near-surface region this description of the oscillations breaks down, because nonadiabatic effects become important. Furthermore, due to the effect of turbulent pressure hydrostatic equilibrium cannot be assumed, at least if p in the above description is taken to be the thermodynamic pressure. It is still possible to define p in the equilibrium model such that eq. (1) is satisfied; but the problem then remains of relating the perturbation of pressure, so defined, to the density perturbation. However, these uncertainties are likely to be confined to a thin region near the surface, as discussed in Section 2.

The observed solar five-minute oscillations are acoustic modes, resulting from interference between acoustic waves which propagate between upper and lower turning points. The location R_t of the upper turning point depends essentially on frequency alone and is given by the condition $\omega = \omega_c(R_t)$, where

$$\omega_c^2 = \frac{c^2}{4H^2}\left(1 - 2\frac{\mathrm{d}H}{\mathrm{d}r}\right), \tag{6}$$

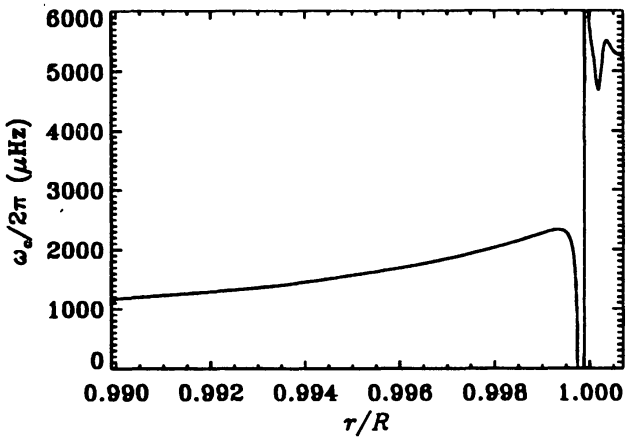

Figure 2. Characteristic frequency ω_c which determines the location of the upper turning point.

H being the density scale height. Figure 2 shows $\omega_c/2\pi$ in the outermost parts of a solar model. For frequencies ν exceeding 2300 μHz R_t is essentially at the photosphere, while for smaller ν the modes are reflected at increasing depth with decreasing frequency. The lower turning point, $r = r_t$, is determined by the condition

$$\frac{\omega}{L} = \frac{c(r_t)}{r_t}\,, \tag{7}$$

with $L = l + 1/2$, and marks the point where the waves undergo total internal reflection, the vertical component of the wave vector being zero. It is evident that modes of high degree are trapped near the surface, while low-degree modes penetrate almost to the centre.

This description of the oscillations leads to a simple expression asymptotically satisfied by the frequencies:

$$\int_{r_t}^{R} \left(1 - \frac{L^2c^2}{\omega^2 r^2}\right)^{1/2} \frac{\mathrm{d}r}{c} = \frac{[n + \alpha(\omega)]\pi}{\omega} \tag{8}$$

(*e.g.* Christensen-Dalsgaard *et al.* 1985; that the observed solar frequencies satisfy a relation of this functional form was first pointed out by Duvall 1982). Here α, which is largely a function of frequency alone, is determined by the properties of the Sun near the upper turning point. Equation (8) illustrates a very important property of the five-minute oscillations: the frequency of a given mode is determined in an integral fashion by the structure of that part of the Sun which lies between the surface and the lower turning point. Since the turning points of the observed modes essentially span the solar radius, it is possible to carry out a localized determination of solar structure based on the observed frequencies. Indeed, eq. (8) may be inverted, to yield the variation $c(r)$ of the solar sound speed, without reference to a solar model.

This model-independent inversion suffers from systematic errors resulting from the asymptotic approximation. Furthermore, one is usually interested in comparing the inferred solar structure with the structure of solar models, to use the results as tests of the

physics and assumptions of the model calculation. Thus, the analysis is often carried out in a differential fashion, in terms of differences between the Sun and a reference model. This assumes that the differences are sufficiently small that the resulting frequency differences are linearly related to the differences in structure. By so linearizing eq. (8) one obtains

$$S_{nl}\frac{\delta\omega_{nl}}{\omega_{nl}} = \mathcal{H}_1\left(\frac{\omega_{nl}}{L}\right) + \mathcal{H}_2(\omega_{nl}) , \tag{9}$$

where

$$\begin{aligned} S_{nl} &= \int_{r_t}^{R}\left(1-\frac{L^2c^2}{r^2\omega_{nl}^2}\right)^{-1/2}\frac{\mathrm{d}r}{c} - \pi\frac{\mathrm{d}\alpha}{\mathrm{d}\omega} , \\ \mathcal{H}_1(w) &= \int_{r_t}^{R}\left(1-\frac{c^2}{r^2w^2}\right)^{-1/2}\frac{\delta_r c}{c}\frac{\mathrm{d}r}{c} , \end{aligned} \tag{10}$$

and $\mathcal{H}_2(\omega) = \delta\alpha(\omega)\pi/\omega$. Here the difference $\delta_r c$ is evaluated at fixed radius r. The function $\mathcal{H}_2(\omega)$ contains contributions from the near-surface region, including the uncertain aspects of the physics. By fitting an expression of the form given in eq. (9) to differences between observed and model frequencies, one may estimate $\mathcal{H}_1(w)$ and thence carry out an inversion to infer $\delta_r c$ (Christensen-Dalsgaard, Gough & Thompson 1989).

Equation (9) assumes that the differences between the Sun and the model are sufficiently small that a linear approximation is adequate and relies on an asymptotic approximation to the frequencies. Maintaining the assumption of small differences but moving beyond the asymptotic approximation, it follows from the discussion above that adiabatic frequency differences can be expressed linearly in terms of differences in two variables, *e.g.* $\delta_r c^2$ and $\delta_r \rho$. However, the actual differences between the observed frequencies and adiabatic frequencies of as model must also reflect the nonadiabatic effects frequencies and the inadequacies in the modelling of the near-surface region. As a result, the frequency differences can be expressed as

$$\frac{\delta\omega_{nl}}{\omega_{nl}} = \int_0^R \left[K^{nl}_{c^2,\rho}(r)\frac{\delta_r c^2}{c^2}(r) + K^{nl}_{\rho,c^2}(r)\frac{\delta_r\rho}{\rho}(r)\right]\mathrm{d}r + E_{nl}^{-1}\mathcal{G}(\omega_{nl}) + \epsilon_{nl} , \tag{11}$$

ϵ_{nl} being the observational error; here the kernels $K^{nl}_{c^2,\rho}$ and K^{nl}_{ρ,c^2} are determined from the eigenfunctions in the model, while the penultimate term arises from the neglected physics in the near-surface region, E_{nl} being the mode inertia normalized by the surface amplitude (*e.g.* Christensen-Dalsgaard & Berthomieu 1991). The form of this term reflects the fact that except at very high degree the vertical scale of the modes near the surface is much smaller than the horizontal scale; consequently the sensitivity of the oscillations to the near-surface errors depends little on degree. The dominant dependence on degree, reflected in the occurrence of E_{nl}, arises from the fact that high-degree modes penetrate less deeply, and therefore have smaller inertia and hence are affected more strongly. It may also be shown that effects confined very close to the surface result in frequency changes which vary slowly with frequency and are small at low frequency.

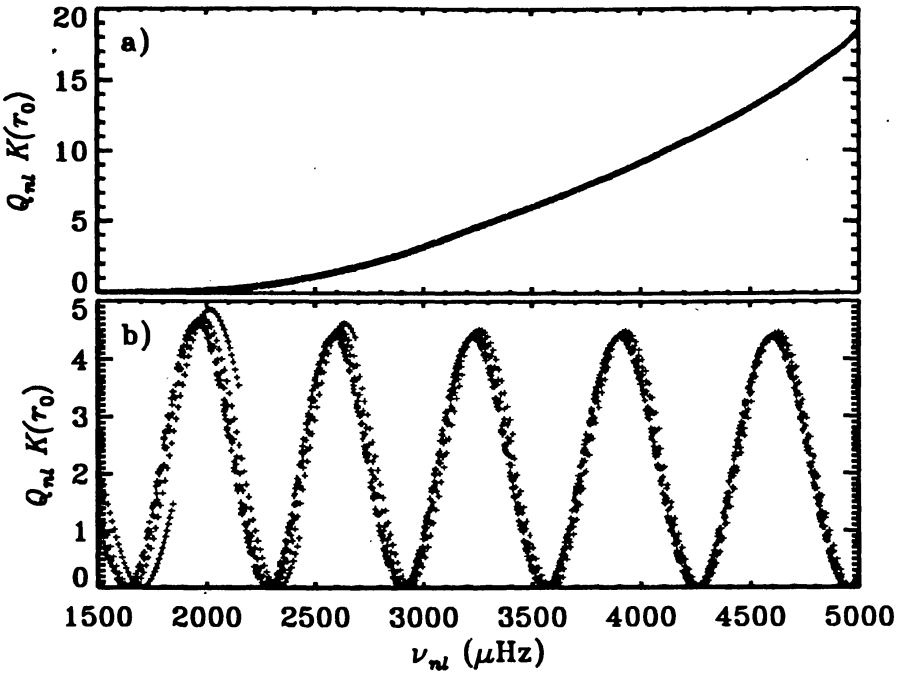

Figure 3. Scaled kernels $K^{nl}_{c^2,\rho}(r_0)$ for modes of degree $l \leq 100$ plotted against frequency for $r_0 = R$ (a) and $r_0 = 0.98R$ (b).

The latter property results from the behaviour of the acoustical cut-off frequency ω_c illustrated in Fig. 2: with decreasing frequency the modes are reflected at increasing depth, and hence the influence of the superficial layers is diminished.

These properties may be illustrated by the behaviour of the kernels $K^{nl}_{c^2,\rho}$ as a function of frequency, for fixed r: it is evident from eq. (11) that this corresponds to the effects on the frequencies of a localized change in the sound speed. To suppress the sensitivity to the mode inertia, the kernels have been scaled by the ratio

$$Q_{nl} = \frac{E_{nl}}{\overline{E}_0(\omega_{nl})}\,, \tag{12}$$

where $\overline{E}_0(\omega)$ is the inertia of radial modes, interpolated to frequency ω. The results are shown in Fig. 3, for several radii r and a range of modes. The very small scatter clearly indicates that that the kernels are in fact largely insensitive to the degree, at fixed frequency. Also, the increasingly oscillatory nature of the kernels with increasing depth is evident. This property can be used to identify contributions to the frequencies arising from sharply localized features in the Sun; important examples are the effects of the rapid variation in Γ_1 in the second helium ionization zone which provides a measure of the convection-zone helium abundance (*e.g.* Vorontsov, Baturin & Pamyatnykh 1991; Pérez Hernández & Christensen-Dalsgaard 1994), and the sharp change in gradients at

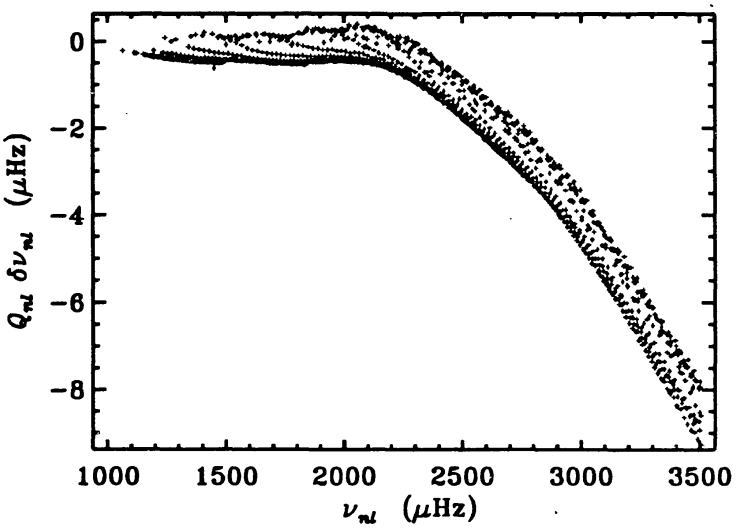

Figure 4. Scaled differences between observed frequencies, obtained with the LOWL instrument (*cf.* Tomczyk, Schou & Thompson, these proceedings), of modes of degree between 0 and 99 and frequencies of a solar model.

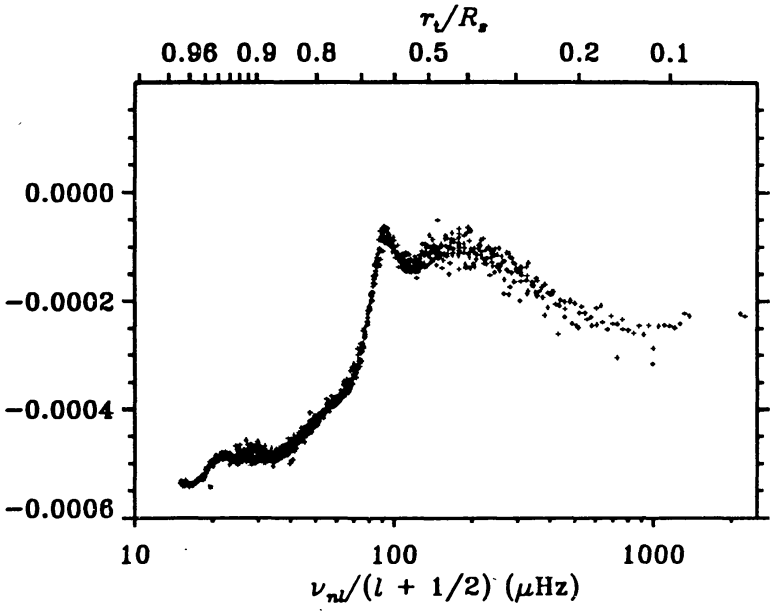

Figure 5. Scaled relative frequency differences, for the case shown in Fig. 4, after subtraction of a fitted function of frequency. The residuals have been plotted against $\nu_{nl}/(l + 1/2)$ and, on the upper abscissa, the corresponding turning-point radius r_t.

the base of the convection zone which may be used to place limits on the extent of the convective overshoot (*e.g.* Basu *et al.* 1994; Monteiro *et al.* 1994).

4. Comparison of observed and computed frequencies

To illustrate the present level of agreement between observed and computed frequencies,

I consider a model computed including the effects of helium and heavy-element settling and diffusion; the equation of state and opacity were obtained from OPAL tables, and the model was calibrated to have solar radius and luminosity, and the observed ratio of heavy-element to hydrogen abundance, at an assumed solar age of 4.6 Gyr. Further details on the model were given by Christensen-Dalsgaard (1996a).

Figure 4 shows frequency differences between the Sun and the model, after scaling by the inertia ratio Q_{nl}. It is evident that the scaled differences depend predominantly on frequency, with little dependence on degree; also, the differences vary slowly with frequency and are small at low frequency. From the discussion in the preceding section it may be concluded that the dominant contributions to the differences arise from errors in the superficial layers of the model. Effects of errors in other parts of the model only become visible if these contributions are eliminated. This may be achieved by carrying out a fit of the form given in eq. (9), to determine the frequency-dependent part of the frequency differences. The residual, after subtraction of this part, has been plotted in Fig. 5 against $\nu/(l+1/2)$ and hence turning-point radius r_t. Clearly there remains a significant contribution, with substantial variation for modes whose turning point is close to the base of the convection zone. As shown by Basu *et al.* (these proceedings) this is associated with a sharp feature in the sound-speed difference in this region.

5. Effects of changes in the model physics

To illustrate the sensitivity of the models and frequencies to changes in the physics, I consider two examples of model changes: a change in the treatment of the superadiabatic gradient; and inclusion of settling of helium and heavy elements. The comparisons are carried out between models calibrated to have solar radius and luminosity, keeping unchanged other aspects than the one explicitly modified.

5.1 Changing the treatment of convection

To illustrate the sensitivity to the near-surface properties of the model, Fig. 6 compares the structure and frequencies of models computed with the Canuto & Mazzitelli and the mixing-length treatments of convection. Panel (a) shows relative differences in squared sound speed and Γ_1, evaluated at fixed interior mass m; such so-called Lagrangian differences provide a truer impression of the physical effect of near-surface changes than do the more commonly used *Eulerian* differences, evaluated at fixed r (*e.g.* Christensen-Dalsgaard & Thompson 1996). It is evident that the differences are indeed confined very near the surface, as a result of the calibration of the models. The steeper temperature gradient in the CM model (*cf.* Fig. 1) leads to a more rapid increase in temperature and hence sound speed; furthermore, the onset of hydrogen ionization is more rapid, leading to a decrease in Γ_1 relative to the MLT model.

The dominant effect on the frequencies comes from the change in ω_c and hence the location of the upper turning point. Neglecting $\mathrm{d}H/\mathrm{d}r$ in eq. (6), $\omega_c \propto \Gamma_1/c$ and hence is decreased in the CM model; this increases the size of the cavity over which the modes propagate and hence decreases the frequencies. As shown in Fig. 6b, the resulting scaled frequency differences are indeed very small at low frequencies and almost independent of l except for $l \gtrsim 300$, as expected. Also, it is interesting that the change is rather

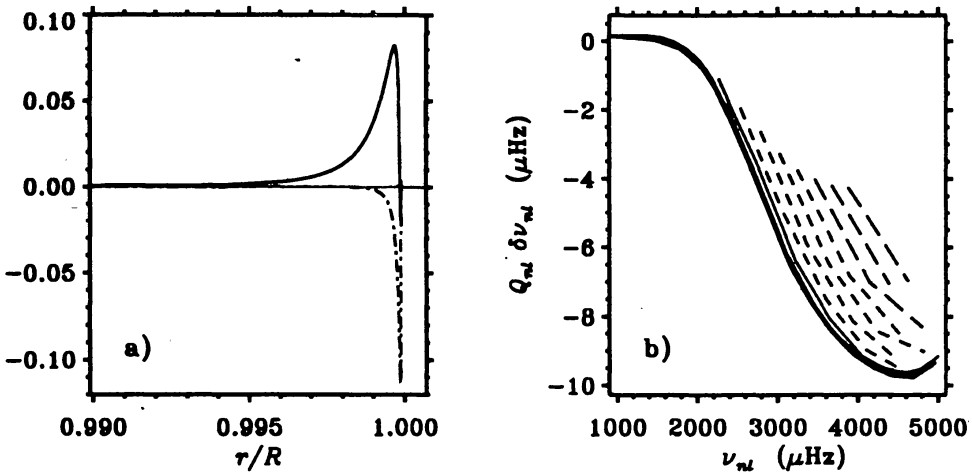

Figure 6. (a) Relative differences in squared sound speed (solid line) and Γ_1 (dot-dashed line) between a model computed with the CM formulation for convection and mixing-length theory, in the sense (CM) – (MLT); the differences were taken at fixed mass. (b) Corresponding scaled frequency differences. Modes of the same degree have been connected by solid lines ($l \leq 300$), short dashed lines ($400 \leq l \leq 700$) and long dashed lines ($800 \leq l$).

similar to the differences between the observed frequencies and those of a MLT model, shown in Fig. 4. This might be taken as support for the CM formulation. It should be noted, however, that rather similar differences can be obtained with a MLT model or from the hydrodynamical simulations, by taking into account the turbulent pressure in the equilibrium model (*e.g.* Rosenthal *et al.* 1995).

5.2 Effects of settling and diffusion

To illustrate the effects on the frequencies of changes in the interior of the model, I consider in Fig. 7 differences between a model including settling and diffusion of helium and heavy elements and a model computed without taking these effects into account. The physics of the model and the ratio between the heavy-element and hydrogen abundances in the model of the present Sun are otherwise the same in the two models. Model differences, at fixed r, are shown in panel (a). Helium settling increases the hydrogen abundance in the convection zone and causes a very steep gradient X just beneath it. The dominant effect in the sound speed is a relatively sharp increase beneath the convection zone, caused largely by the fact that the convection zone is somewhat deeper in the model with settling. There are also smaller effects in the ionization zones of hydrogen and helium, caused by the change in Γ_1 resulting from the change in composition.

To illustrate the effects of these changes on the frequencies, the scaled frequency differences have been separated into a part depending on the turning-point location and a part depending on frequency, in the manner of eq. (9). As shown in Fig. 7b, the former part is dominated by the positive difference in c just beneath the convection zone, which causes a sharp increase in the frequencies of the modes penetrating beyond this point. It is striking that this effect is larger by a factor of more than four than the corresponding component of the differences, shown in Fig. 5, between the observed

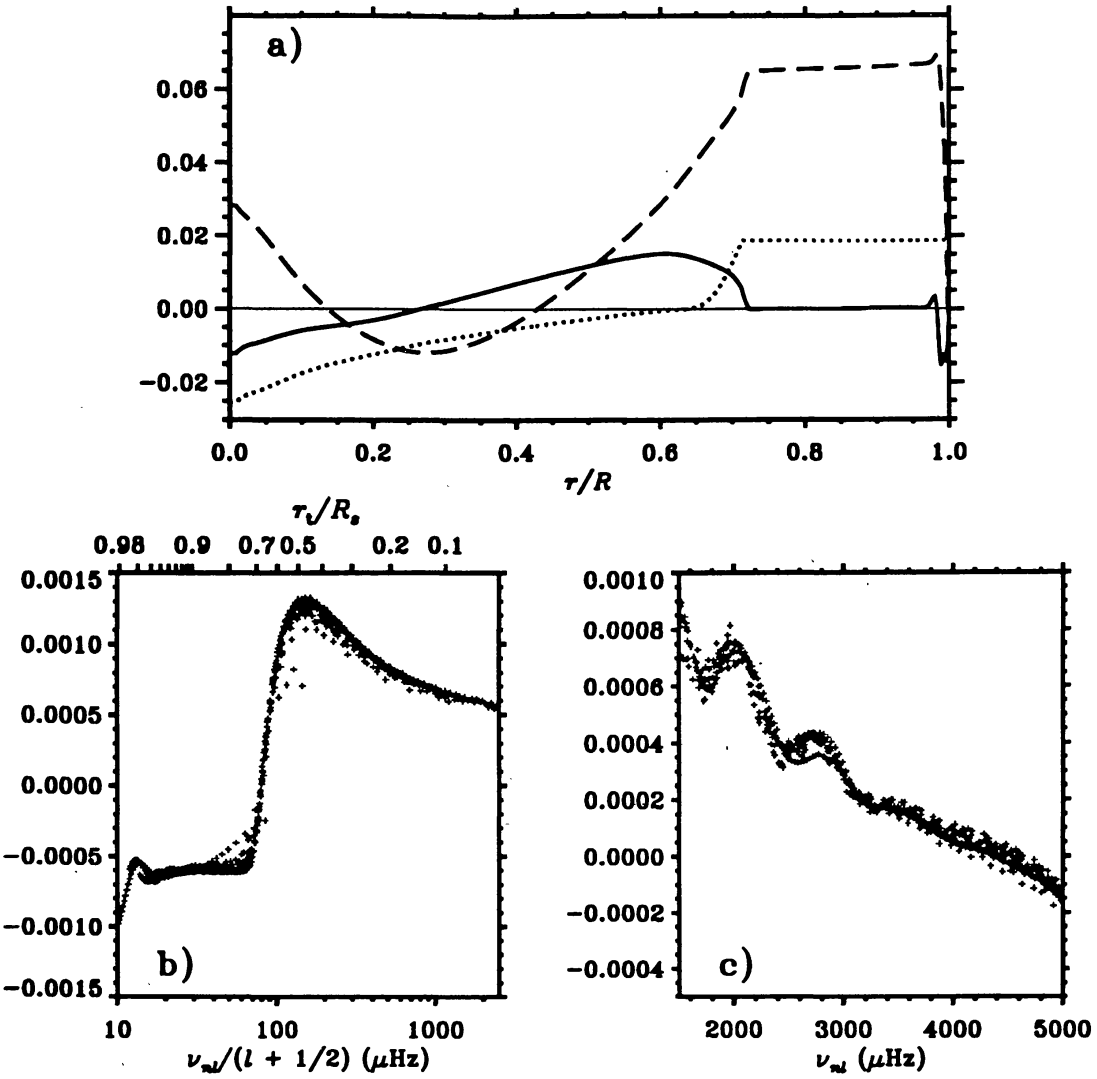

Figure 7. (a) Relative differences, at fixed radius, in squared sound speed (solid line) and density (dashed line), and difference in hydrogen abundance X (dotted line), between a model including settling and a model neglecting it, in the sense (settling) − (no settling). (b) Corresponding scaled relative frequency differences $Q_{nl}\delta\nu_{nl}/\nu_{nl}$, after subtraction of the frequency-dependent part corresponding to the term $\mathcal{H}_2(\omega)$ in eq. (9). (c) Scaled relative frequency differences, after subtraction of the part corresponding to the term $\mathcal{H}_1(\omega/L)$ in eq. (9).

frequencies and frequencies of a model including settling; this is strong evidence that settling must be taken into account in solar modelling, as is also found from inversion of the frequency differences (see Basu *et al.*, these proceedings). The frequency-dependent part shows a clear oscillatory signal, which, based on its period, can be attributed to the second helium ionization zone (*cf.* the discussion of Fig. 3), and is caused by the difference in envelope composition between the two models. Such oscillatory signals have in fact been used to infer the solar envelope helium abundance (*e.g.* Pérez Hernández & Christensen-Dalsgaard 1994).

6. Conclusions

The examples presented here only provide an superficial indication of the sensitivity of the solar oscillation frequencies to aspects of solar structure. Other examples are discussed elsewhere in these proceedings, and an extensive set was provided by Christensen-Dalsgaard (1996b). Thanks to extreme precision with which the frequencies can be observed and the variety of modes that are available we can probe subtle aspects of both the micro- and the macrophysics. It is perhaps surprising that models computed *ab initio*, with no attempt to match the data, are so successful in reproducing solar structure as inferred helioseismically. However, the remaining discrepancies clearly indicate that improvements are needed, very likely involving phenomena that have so far been ignored in stellar modelling and leading to a deeper insight into both the properties of stellar evolution and the physical processes that control it.

References

Ahrens, B., Stix, M. & Thorn, M., 1992. *Astron. Astrophys.*, **264**, 673

Anders, E. & Grevesse, N., 1989. *Geochim. Cosmochim. Acta*, **53**, 197

Basu, S., Antia, H. M. & Narasimha, D., 1994. *Mon. Not. R. astr. Soc.*, **267**, 209

Canuto, V. M. & Mazzitelli, I., 1991. *Astrophys. J.*, **370**, 295

Chaboyer, B., Demarque, P. & Pinsonneault, M. H., 1995. *Astrophys. J.*, **441**, 865

Christensen-Dalsgaard, J., 1996a. In *Proc. Workshop on Theoretical and Phenomenological Aspects of Underground Physics (TAUP'95)*, ed. Fatas, M., *Nucl. Phys. B, Suppl.*, in the press.

Christensen-Dalsgaard, J., 1996b. In *Proc. VI IAC Winter School "The structure of the Sun"*, ed. T. Roca Cortes, Cambridge University Press, in the press.

Christensen-Dalsgaard, J. & Berthomieu, G., 1991. In *Solar interior and atmosphere*, p. 401 eds Cox, A. N., Livingston, W. C. & Matthews, M., Space Science Series, University of Arizona Press.

Christensen-Dalsgaard, J. & Thompson, M. J., 1996. *Mon. Not. R. astr. Soc.*, submitted.

Christensen-Dalsgaard, J., Duvall, T. L., Gough, D. O., Harvey, J. W. & Rhodes Jr, E. J., 1985. *Nature*, **315**, 378

Christensen-Dalsgaard, J., Gough, D. O. & Thompson, M. J., 1989. *Mon. Not. R. astr. Soc.*, **238**, 481

Christensen-Dalsgaard, J., Gough, D. O. & Thompson, M. J., 1991. *Astrophys. J.*, **378**, 413

Christensen-Dalsgaard, J., Gough, D. O. & Thompson, M. J., 1992. *Astron. Astrophys.*, **264**, 518

Cox, A. N., Guzik, J. A. & Kidman, R. B., 1989. *Astrophys. J.*, **342**, 1187

Dilke, F. W. W. & Gough, D. O., 1972. *Nature*, **240**, 262

Duvall, T. L., 1982. *Nature*, **300**, 242

Montalbán, J., 1994. *Astron. Astrophys.*, **281**, 421

Monteiro, M. J. P. F. G., Christensen-Dalsgaard, J. & Thompson, M. J., 1994. *Astron. Astrophys.*, **283**, 247

Noerdlinger, P. D., 1977. *Astron. Astrophys.*, **57**, 407

Pérez Hernández, F. & Christensen-Dalsgaard, J., 1994. *Mon. Not. R. astr. Soc.*, **269**, 475

Press, W. H. & Rybicki, G. B., 1981. *Astrophys. J.*, **248**, 751

Rosenthal, C. S., Christensen-Dalsgaard, J., Houdek, G, Monteiro, M.J.P.F.G., Nordlund, Å. & Trampedach, R., 1995. In *Proc. Fourth SOHO Workshop: Helioseismology*, eds Hoeksema, J. T., Domingo, V., Fleck, B & Battrick, B., ESA SP-376, vol. 2, ESTEC, Noordwijk, p. 459

Schatzman, E., Maeder, A., Angrand, F. & Glowinski, R., 1981. *Astron. Astrophys.*, **96**, 1

Schmitt, J. H. M. M., Rosner, R. & Bohn, H. U., 1984. *Astrophys. J.*, **282**, 316

Stein, R. F. & Nordlund, Å., 1989. *Astrophys. J.*, **342**, L95

Vorontsov, S. V., Baturin, V. A. & Pamyatnykh, A. A., 1991. *Nature*, **349**, 49

Wambsganss, J., 1988. *Astron. Astrophys.*, **205**, 125

Zahn, J.-P., 1991. *Astron. Astrophys.*, **252**, 179